

Calibration of an NMR system for measuring ^3He polarization

A thesis submitted in partial fulfillment of the requirement
for the degree of Bachelor of Science with Honors in
Physics from the College of William and Mary in Virginia,

by

Marc McGuigan

Accepted for _____

Advisor: Dr. Todd D. Averett

Dr. Christopher D. Carone

Dr. Gina L. Hoatson

Dr. Junping Shi

Williamsburg, Virginia
April 2003

Abstract

Scientists around the world use ^3He to study the spin structure of the neutron. This study is made more efficient by polarizing ^3He through a process of spin-exchange collisions with optically pumped alkali vapor. One method to determine the absolute ^3He polarization employs the techniques of nuclear magnetic resonance. Water has a known polarization and serves as a standard by which to calibrate the polarization of a given sample. If a water sample is placed in two magnetic fields, one constant and one oscillating with time, the spins of the water molecules absorb energy at a certain resonant frequency. When the spins flip, a voltage is induced in nearby pickup coils. This process is repeated with a ^3He sample. Together, the two NMR signals and the polarization of water are used to determine the polarization of the ^3He sample. Using this method, the absolute polarization of a ^3He target cell, Voltaire, was measured to be $(8.1 \pm 1.0)\%$.

Acknowledgements

There were many people who helped make this research experience both educational and fun. I would like to thank Vincent Sulkosky for taking the time to explain the flux factor and coil modeling. Despite his busy schedule, Vince always found the time to respond to my emails and point me in the right direction. I would like to thank Kevin Kramer for helping me fit the water signal. I would like to thank Kirsten Fuoti for helping me with LabView and for being an all around outstanding lab partner. Finally, I would like to thank my advisor Dr. Todd Averett for his guidance and support. He was always available to answer my questions and he was an invaluable resource throughout the whole year. Without his help this project would not have been possible.

Contents

Abstract	2
Acknowledgements	3
1 Introduction	5
2 Polarization	8
2.1 Theory.....	8
2.1.1 Optical Pumping.....	8
2.1.2 Spin Exchange.....	10
2.2 Experimental Setup.....	11
2.2.1 Target Cells.....	11
2.2.2 Target System.....	13
3 Nuclear Magnetic Resonance	15
3.1 Precession.....	15
3.1.1 Quantum Precession.....	15
3.1.2 Classical Precession.....	18
3.1.3 Precession in Rotating Fields.....	20
3.1.4 Adiabatic Fast Passage.....	21
3.2 Measuring a ^3He Signal.....	22
4 Water Calibration	26
4.1 Spin Relaxation.....	26
4.2 Polarization of Water.....	29
4.3 Magnetic Moment and Experimental Constants.....	30
4.4 Flux Factor.....	31
4.4.1 Geometric Flux.....	31
4.4.2 Coil Modeling.....	33
4.5 Measuring a Water Signal.....	37
4.6 Calibrating the System.....	39
4.7 Treatment of Errors.....	40
5 Conclusion	44
Appendix	45
References	46

Chapter 1

Introduction

Nuclear physicists throughout the world are constantly using innovative techniques to investigate the nuclear properties of the universe. The study of the neutron spin structure using ^3He is a good example of such research. Through experimentation, researchers have provided the scientific community with a more complete understanding of the subatomic particles, forces, and interactions that exist within the neutron. In addition, studying polarized ^3He has led to significant advancements in fields such as medical imaging [1].

Studying the neutron is challenging because free neutrons are unstable; they have a half-life of 10.23 ± 0.01 minutes [2]. To address this problem, researchers have found that ^3He serves as a good substitute for the free neutron. The nucleus of a ^3He atom is composed of two protons and one neutron [3]. There is a 90% chance that the nucleus will be in the S state; the proton spins will be anti-aligned and the neutron spin will determine the polarization of the entire nucleus (*Figure 1*). There is an 8% chance that the atom will be found in the D state; the proton spins are aligned with the neutron spin. Finally, there is a 2% chance that the atom will be found in the S' state; the proton spins are aligned but they are anti-aligned with neutron spin. Since ^3He is most

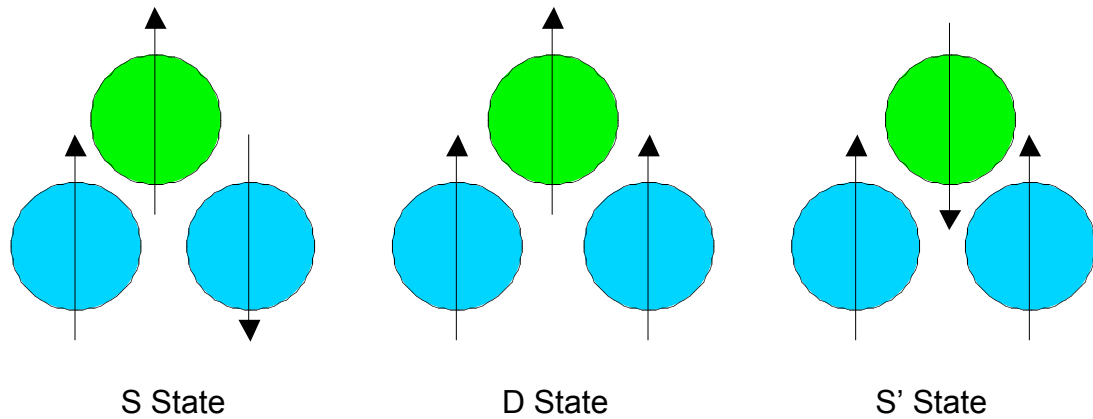


Figure 1: Spin states of the ^3He nucleus.

Note: Protons are shaded blue and the neutron is shaded green.

likely to be in the S state, the neutron spin usually determines the polarization of the entire nucleus. The challenge, however, is to align or polarize the spins of every ^3He nucleus in the target. Increasing the polarization of the ^3He atoms allows scientists to make more precise neutron structure measurements.

Researchers at the Thomas Jefferson National Accelerator Facility (TJNAF) in Newport News, Virginia have conducted many experiments to study the neutron spin structure [4, 5, 6]. At TJNAF, an electron beam passes through a glass cell filled with ^3He . The beam collides with the ^3He atoms and the scattering that results can be analyzed using detectors. For a given amount of time, the error from the scattering data collected is inversely proportional to the square of the polarization of the ^3He target [7].

Research is taking place at the College of William and Mary to create and polarize ^3He target cells to be used at Jefferson Lab. This past year the polarized ^3He research at William and Mary has focused on attaining a high level of polarization in a

^3He target cell and calculating the absolute polarization of a ^3He target cell. This Honors project focuses on the second of these goals, calculating the absolute polarization of a ^3He target cell.

Chapter 2

Polarization

2.1 Theory

2.1.1 Optical Pumping

A ^3He nucleus is polarized through a process optical pumping and spin exchange [8]. The process involves three gases: Rb, N_2 , and ^3He . First, rubidium is heated into a gas state. Then, rubidium in the $5S_{\downarrow}$ atomic state is placed in the presence of a magnetic field. A Zeeman splitting will result, creating two electron states $m = -_{\downarrow}$ and $m = +_{\downarrow}$ (*Figure 2*). Circularly polarized light, with a wavelength of 795 nm interacts with the Rb, exciting it into the $5P_{\downarrow}, m = +_{\downarrow}$ state. As a result of the excited rubidium atoms colliding with other atoms in the gas (collisional mixing), the electrons originally in the $5P_{\downarrow}, m = +_{\downarrow}$ atomic state will be distributed equally between the $m = -_{\downarrow}$ and $m = +_{\downarrow}$ atomic states. The electrons can then decay back to the $5S_{\downarrow}, m = -_{\downarrow}$ state and the $5S_{\downarrow}, m = +_{\downarrow}$ state with equal probability. Those rubidium atoms that decay to the $m = -_{\downarrow}$ state may once again be excited by circularly polarized light, thus repeating the process. If, however, the rubidium decays to the $m = +_{\downarrow}$ state it can no longer be excited. Over time, all of the rubidium atoms become trapped in the spin up state.

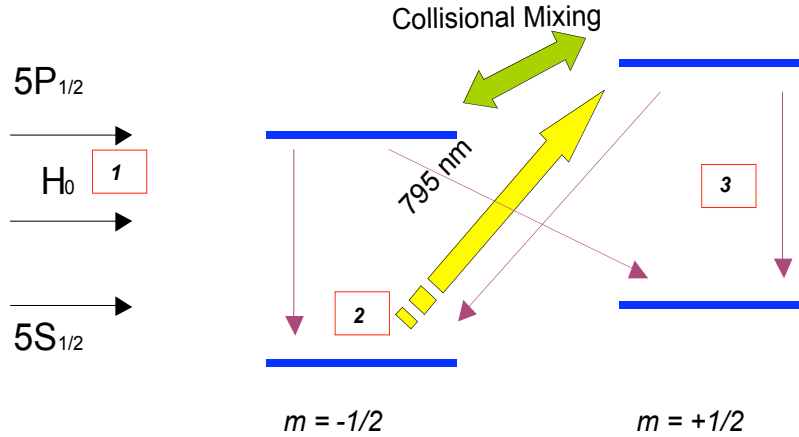


Figure 2: Optical Pumping.

- 1.) A static magnetic field, H_0 , creates a Zeeman splitting of the electron states.
- 2.) Circularly polarized light excites outer shell electrons from the $5S_{-}$ state to the $5P_{-}$ state.
- 3.) The electrons decay back to the $5S_{-}$ $m = -_{-}$ and $m = +_{-}$ state with equal probability by emitting a photon (purple arrows).

Nitrogen molecules (N_2) also play a role in the polarization of ^3He [8]. When a rubidium atom decays from the $5P_{-}$ state to the $5S_{-}$ state a photon is released. The emitted photon has a random polarization and it may be reabsorbed by another rubidium atom. Since it is unlikely that this photon will have the correct polarization direction, the rubidium will not have the correct spin direction, thus reducing the efficiency of the optical pumping process.

Approximately 60 torr of N_2 is added to the system to prevent the negative effects of the reabsorbed photons. The N_2 molecule is able to absorb the energy from the excited atoms into its rotational and vibrational motion [8]. This process is known as quenching and allows for a high rubidium polarization.

2.1.2 Spin Exchange

When polarized rubidium and ^3He collide in the target cell, the rubidium wavefunction overlaps with the nuclear wavefunction of the ^3He atom [9]. This hyperfine-like interaction causes a spin exchange between the rubidium atom and the ^3He nucleus in which angular momentum is transferred



Following this process, the rubidium is quickly polarized again, allowing the process to be repeated. The nuclear spin, however, remains in the up position as long as no depolarization effects are present. The ^3He polarization with respect to time can then be calculated [8]

$$P_{\text{He}}(t) = \langle P_{\text{Rb}} \rangle \frac{\Gamma_{\text{SE}}}{\Gamma_{\text{SE}} + \Gamma} \left(1 - e^{-\Gamma_{\text{SE}} t} \right) \quad (2.2)$$

$\langle P_{\text{Rb}} \rangle$ is the average polarization of rubidium, Γ is the ^3He nuclear spin relaxation rate, and Γ_{SE} is the ^3He - Rb spin exchange rate by which the rubidium transfers spin to ^3He . Over long periods of time this becomes [7]

$$P_{\text{He}}^{\text{Final}} = \frac{\Gamma_{\text{SE}}}{\Gamma_{\text{SE}} + \Gamma} \langle P_{\text{Rb}} \rangle \quad (2.3)$$

Some of the factors that may cause an increase in the relaxation rate, Γ are an inhomogeneous magnetic field, $^3\text{He} - ^3\text{He}$ magnetic dipole interactions, collisions with gas impurities, and wall collisions with impurities in the target cell [10].

2.2 Experimental Setup

2.2.1 Target Cells

The target cell is the physical enclosure that holds the ^3He , Rb, and N_2 . Target cells at the College of William and Mary are made of General Electric type 180, aluminosilicate glass [10]. Aluminosilicate glass has a low porosity to ^3He , a characteristic that is believed to help achieve a high level of polarization. Before a cell is filled it is connected to a vacuum system to pump out any impurities. Each cell includes a target chamber, the transfer tube, and the pumping chamber (*Figure 3*).

The target chamber is typically 40 cm long with a diameter of approximately 2 cm. Each end of the chamber has a curved end window approximately 140 microns thick, and the side walls are about 1 mm thick [7]. When experiments are conducted at an accelerator facility, the target cell is placed in the path of the electron beam such that it enters the first end window and passes out the other (unless it is scattered through the walls). The scattering between the beam and ^3He atoms takes place in the target chamber.

The transfer tube is approximately 6 cm long and 1.2 cm in diameter, and connects the target chamber to the pumping chamber. The pumping chamber is a sphere with a diameter of about 6.3 cm. In the presence of laser light, rubidium optical pumping and spin exchange takes place in the pumping chamber.

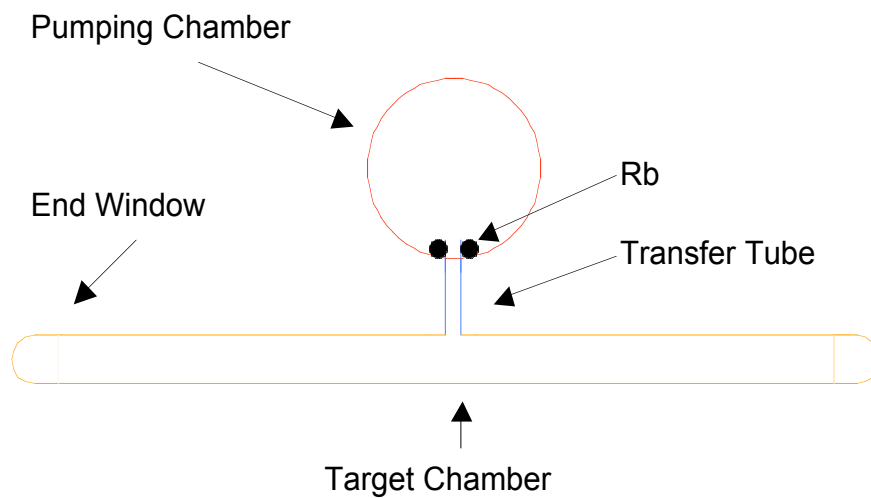


Figure 3: Target Cell

Rubidium is placed at the bottom of the pumping chamber so that optical pumping and spin exchange may take place. The target chamber is outlined in orange, the transfer tube is outlined in blue, and the pumping chamber is outlined in red.

Most cells are filled with 8.5 amagats of ^3He and are used in experiments at TJNAF. Some cells are filled with water and are used to calibrate the Nuclear Magnetic Resonance system.

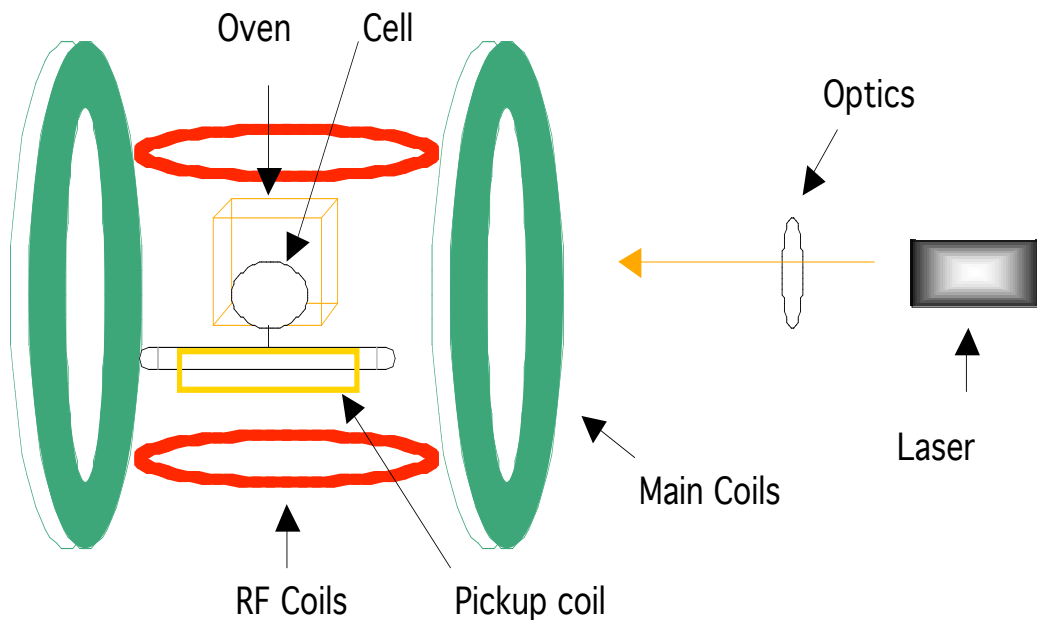


Figure 4: Target System

Note: There is a pickup coil on each side of the cell; only one is visible from this view.

2.2.2 Target System

Once a target cell is filled (with ^3He or water) it is mounted such that the pumping chamber is enclosed within an oven (*Figure 4*), which measures 4.25", by 4.25", by 5.125"[7]. The oven heats the rubidium to 170°C, the optimum temperature required for optical pumping to take place. The temperature in the system is measured using a resistance temperature detector (RTD).

A set of pickup coils is adjacent to, and parallel with, the target chamber of the cell. Laser light from a Coherent FAP 30 W Diode Laser passes through polarizing optics before reaching the pumping chamber of the cell [7]. The light is circularly

polarized and has a wavelength of 795 nm so that the optical pumping process may take place.

Two sets of Helmholtz coils create the magnetic fields necessary for the polarization process and subsequent Nuclear Magnetic Resonance measurements. The first set has an inner diameter of 57" and an outer diameter of 62" [7]. This large set of coils creates a homogeneous magnetic holding field that is swept from 25 G to 32 when testing a ^3He sample and from 18 G to 25 G when testing a water sample. The second set of coils (the RF coils) is orthogonal to the larger set and has an inner diameter of 31" and an outer diameter of about 34". The coils create an RF field at 91 kHz.

Chapter 3

Nuclear Magnetic Resonance

3.1 Precession

3.1.1 Quantum Precession

Once ^3He nuclei are polarized, the level of polarization can be measured using Nuclear Magnetic Resonance (NMR). In order to fully explain the theory of NMR the discussion will begin by analyzing one magnetic dipole in a static magnetic field.

Consider one neutron in the presence of a constant magnetic field, $\vec{H}_0 = H_0 \hat{z}$ [11]. The Hamiltonian of such a system is:

$$\text{Hamiltonian} = \gamma H_0 S_z = \frac{\gamma H_0 \hbar}{2} \begin{pmatrix} 1 & 0 \\ 0 & -1 \end{pmatrix} \quad (3.1)$$

In equation (3.1), γ is the gyromagnetic ratio. The eigenstates of H_0 denoted, χ_{\uparrow} , and χ_{\downarrow} ,

$$\chi_{\uparrow} = \begin{pmatrix} 1 \\ 0 \end{pmatrix} \quad (3.2)$$

$$\chi_{\downarrow} = \begin{pmatrix} 0 \\ 1 \end{pmatrix} \quad (3.3)$$

have corresponding energies:

$$E_+ = \frac{(\hbar H_0 \hbar)}{2} \quad (3.4)$$

$$E_- = \frac{(\hbar H_0 \hbar)}{2} \quad (3.5)$$

Consider the solution to the time independent Schrödinger equation:

$$\psi(t) = a\psi_+ e^{\frac{iE_+t}{\hbar}} + b\psi_- e^{\frac{iE_-t}{\hbar}} \quad (3.6)$$

$$\psi(t) = \begin{bmatrix} ae^{\frac{iH_0t}{2}} \\ be^{\frac{iH_0t}{2}} \end{bmatrix} \quad (3.7)$$

The constant coefficients, a and b , can be determined by the initial condition in which:

$$|a|^2 + |b|^2 = 1 \quad (3.8)$$

Two values that fit such conditions are:

$$a = \cos\left(\frac{\theta}{2}\right) \quad (3.9)$$

$$b = \sin\left(\frac{\theta}{2}\right) \quad (3.10)$$

$$\psi(t) = \begin{bmatrix} \cos\left(\frac{\theta}{2}\right) e^{\frac{iH_0t}{2}} \\ \sin\left(\frac{\theta}{2}\right) e^{\frac{iH_0t}{2}} \end{bmatrix} \quad (3.11)$$

The expectation value of the spin yields interesting results:

$$\langle S_x \rangle = \frac{\hbar}{2} \sin(\theta) \cos(\theta H_0 t) \quad (3.12)$$

$$\langle S_y \rangle = \frac{\hbar}{2} \sin(\theta) \sin(\theta H_0 t) \quad (3.13)$$

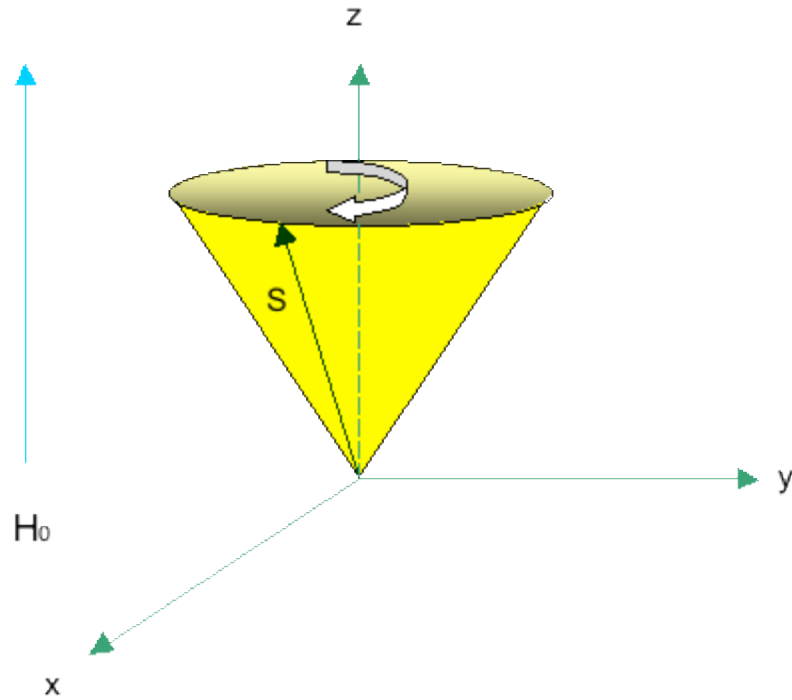


Figure 5: Larmor Precession of the magnetic dipole spin in the presence of a constant magnetic field $\vec{H} = H_0 \hat{z}$.

$$\langle S_z \rangle = \frac{\hbar}{2} \cos(\theta) \quad (3.14)$$

Thus, the spin precesses at an angle θ about the z direction. This is a Larmor precession and occurs with a frequency (*Figure 5*)

$$\omega_0 = \gamma H_0 \quad (3.15)$$

Now, again consider the neutron as a magnetic dipole in a constant magnetic field, $\vec{H} = H \hat{z}$ [7]. The magnetic dipole moment is

$$\vec{\mu} = \gamma \hbar \vec{J} \quad (3.16)$$

The total angular momentum (spin and orbital angular momentum of the nucleus) is $\hbar\vec{J}$.

The energy of this dipole moment is

$$E = \vec{\mu} \cdot \vec{H} = \mu H_0 \hbar J_z \quad (3.17)$$

Since $J_z = \pm 1$, the difference in energy between the states is

$$\Delta E = \hbar \Delta = \mu H_0 \quad (3.18)$$

The frequency of the photon required for this transition is

$$\Delta_0 = \Delta H_0 \quad (3.19)$$

3.1.2 Classical Precession

Thus far, quantum mechanics has been used to understand how the neutron would react to the presence of a magnetic field. It will now be demonstrated that, although the neutron lives at the quantum scale, in this case, it acts in a manner that is consistent with classical theory [12]. Equation (3.16) states that

$$\vec{\mu} = \mu \vec{J} \quad (3.16)$$

The magnetic field exerts a torque on this dipole

$$\vec{\tau} = \frac{d(\hbar\vec{J})}{dt} \quad (3.20)$$

$$\vec{\tau} = \vec{\mu} \times \vec{H} \quad (3.21)$$

By combining equation (3.16), equation (3.20), and equation (3.21)

$$\frac{d\vec{\mu}}{dt} = \mu (\vec{\mu} \times \vec{H}) \quad (3.22)$$

At this point, it is conventional to transform equation (3.22) into a coordinate system rotating with angular velocity ω . In this frame of reference

$$\frac{d\psi}{dt} = \frac{\partial\psi}{\partial t} + (\omega \psi) \quad (3.23)$$

$$\frac{\partial\psi}{\partial t} = \frac{\partial\psi}{\partial t} + \omega \psi + \frac{\partial\psi}{\partial t} \quad (3.24)$$

If the frame rotates in the counter-clockwise direction with respect to the magnetic field direction, $\omega = \omega(\hat{H})$ so [7]

$$\frac{\partial\psi}{\partial t} = \frac{\partial\psi}{\partial t} + \omega H_0 \psi + \frac{\partial\psi}{\partial t} \hat{H} \quad (3.25)$$

If one lets $\omega = \omega H_0$ then

$$\frac{\partial\psi}{\partial t} = 0 \quad (3.26)$$

This means that in the laboratory frame the system precesses with a Larmor frequency

$$\omega = \omega H_0 \quad (3.27)$$

This is the same frequency that was calculated in equation (3.15) and equation (3.19).

This is interesting for two reasons. First, when another magnetic field is applied to the system with a frequency that matches the frequency of the Larmor precession, a spin flip takes place. Second, although the magnetic dipole moment of a neutron is often treated in a quantum mechanical manner, in this situation the quantum results resemble the results of a classical approach. Consequently much of the analysis from this point will take place within a classical framework.

3.1.3 Precession in Rotating Fields

The previous two sections discussed how a magnetic dipole would act in the presence of a constant magnetic field oriented in one direction. If a rotating component $H_1(\cos(\omega_1 t)\hat{x} + \sin(\omega_1 t)\hat{y})$ is added it is useful to move into a reference frame that is rotating with a frequency $\omega_1 = \omega_1\hat{z}$ [7]. In this frame the magnetic field is

$$\vec{H} = H_0\hat{z} + H_1\hat{x} \quad (3.28)$$

Reference [7] provides a detailed account of the change of coordinates. This system has an effective magnetic field

$$\vec{H}_{eff} = \left[H_0 - \frac{\omega_1}{\gamma} \right] \hat{z} + H_1\hat{x} \quad (3.29)$$

In the rotating frame, the magnetic moment will precess around the effective magnetic field with a frequency

$$\omega = \gamma H_{eff} \quad (3.30)$$

Resonance occurs at

$$\omega_1 = \omega H_0 \quad (3.31)$$

when the magnetic moment precesses around the \hat{x} axes. When the system is not in resonance $|H_1| \ll |H_0|$ and the rotation is about the \hat{z} axes.

If an oscillating magnetic field is applied, \vec{H}_1 (RF coils generate such a field) the system can be treated as if there were two magnetic fields rotating in opposite directions [7,13].

$$\vec{H}_1 = H_1 \left((\cos(\omega_1 t)\hat{x} + \sin(\omega_1 t)\hat{y}) + (\cos(\omega_1 t)\hat{x} - \sin(\omega_1 t)\hat{y}) \right) \quad (3.32)$$

In this system it is only necessary to consider the effects of one rotating field, rotating at a frequency, $\omega_1 = \omega_1 \hat{z}$ because in the frame of this rotation the other field is has a frequency of $2\omega_1 \hat{z}$, a value that is not near the resonance condition. Thus the system reduces to the case described earlier with only one magnetic field. At resonance, $\vec{H}_{eff} = H_1 \hat{x}$.

3.1.4 Adiabatic Fast Passage

Adiabatic fast passage is a technique in which a homogeneous magnetic field, \vec{H}_0 in the presence of an oscillating magnetic field, \vec{H}_1 is swept through a resonance frequency. At the resonance frequency the magnetization of the gas induces an EMF in nearby pickup coils. The process must sweep at a rate such that the magnetization can follow the effective magnetic field [13]. When considering this condition, it is useful to deal with the most extreme situation, at resonance, when $H_{eff} = H_1$. If the time passage through resonance is

$$\Delta = \frac{H_1}{\left| \frac{dH_0}{dt} \right|} \quad (3.33)$$

the adiabatic condition is then

$$\frac{1}{H_1} \left| \frac{dH_0}{dt} \right| \ll \Delta H_1 \quad (3.34)$$

However, while the sweep must not run too fast, if it sweeps too slow the magnetization is lost due to spin relaxation. T_1 and T_2 refer to the longitudinal and transverse relaxation

times respectively. The T_1 constant measures the rate that an excited system will return to the ground state [13]. The T_2 time constant is not due to an energy exchange but rather a loss of phase coherence among spins, very often due to an applied magnetic field that is not perfectly homogeneous. The T_2 constant is usually less than T_1 . Combining both the “adiabatic” and the “fast” conditions AFP requires

$$\frac{1}{T_1} \ll \frac{1}{H_1} \left| \frac{dH_0}{dt} \right| \ll \omega H_1 \quad (3.35)$$

The T_1 time for ^3He is approximately 100 seconds [14].

3.2 Measuring a ^3He Signal

In the rotating frame, the \hat{x} component of the magnetization can be calculated [13]

$$M_{x\hat{}} = \omega NP \hat{H}_{eff} \cdot \hat{x}\hat{} \quad (3.36)$$

where N is the number of spins and P is the polarization. Using the unit vector of equation (3.27)

$$\hat{H}_{eff} = \frac{H_1 \hat{x}\hat{} + \omega H_0 \frac{\omega}{\omega} \hat{z}\hat{}}{\sqrt{H_1^2 + \omega H_0 \frac{\omega}{\omega}}^2} \quad (3.37)$$

the $\hat{x}\hat{}$ component of the magnetic field is

$$M_{x\hat{}} = \omega NP \frac{H_1}{\sqrt{H_1^2 + \omega H_0 \frac{\omega}{\omega}}^2} \quad (3.38)$$

This magnetization will induce an EMF in the pickup coils. This EMF is measured using electronics as well as computer software and the signal height is proportional to the magnetization. The signal will have the form

$$S_{ind} = S_{peak} \frac{H_1}{\sqrt{H_1^2 + \left(\frac{H_0}{Q} \right)^2}} \quad (3.39)$$

The peak amplitude of the ^3He signal can be modeled using

$$S_{^3\text{He}} \propto \mu_{^3\text{He}} n_{^3\text{He}} P_{^3\text{He}} \left(\frac{geo}{^3\text{He}} \right) G_{^3\text{He}} \quad (3.40)$$

when $\mu_{^3\text{He}}$ is the magnetic moment of ^3He , $n_{^3\text{He}}$ is the density of the ^3He sample, $P_{^3\text{He}}$ is the ^3He polarization, $\left(\frac{geo}{^3\text{He}} \right)$ is the geometric flux factor that accounts for the cell geometry and cell placement between the pickup coils, and $G_{^3\text{He}}$ is the electronic gain in the system during the ^3He measurement.

At the College of William and Mary, polarization signals are measured using NMR electronics and computer software [7]. An RF function generator applies a voltage to an RF amplifier, producing a 91 kHz RF magnetic field. The two main coils create a holding field that sweeps at a rate of $1.2 \frac{\text{G}}{\text{s}}$. It first ramps up from 25 G to 32 G and then ramps down from 32 G to 25 G. Resonance occurs around 28 Gauss. A Perkin-Elmer 7265 Lock-in Amplifier is used to measure the output voltage from the preamp at a certain frequency.

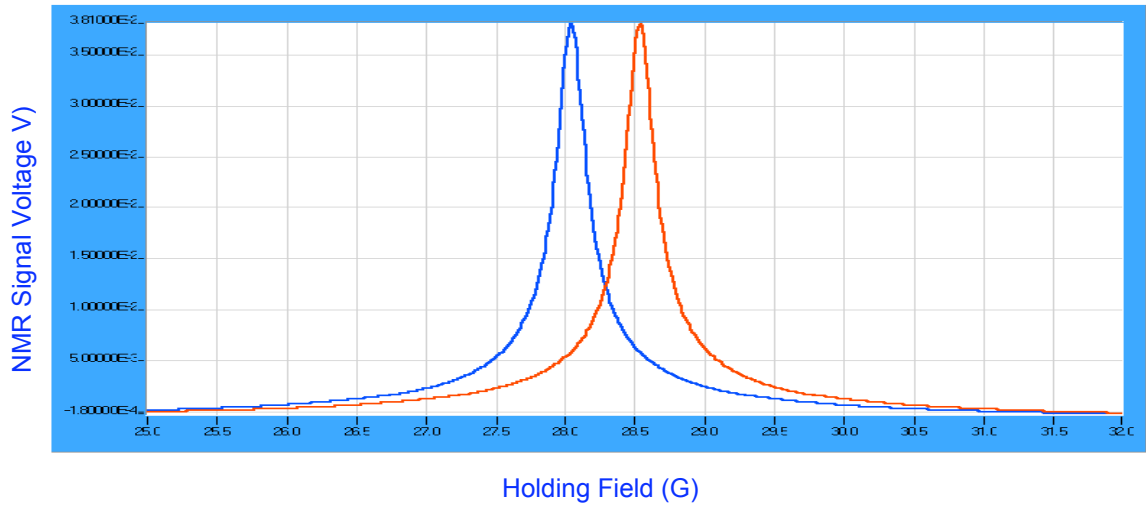


Figure 6: AFP Polarization Signal for Voltaire

Note: The up sweep is outlined in red and the down sweep is outlined in blue

The AFP polarization signal was measured for a ^3He cell named Voltaire. (*Figure 6*).

The up sweep was fit using computer software. The maximum peak height was determined to be 39.5 mV (*Figure 7*). When Voltaire was filled the density of ^3He was $n_{^3\text{He}} = 8.5$ amg, however since the oven is heated to 170°C during optical pumping, the density of ^3He between the pickup coils increased to $n_{^3\text{He}} = 10.2$ amg.

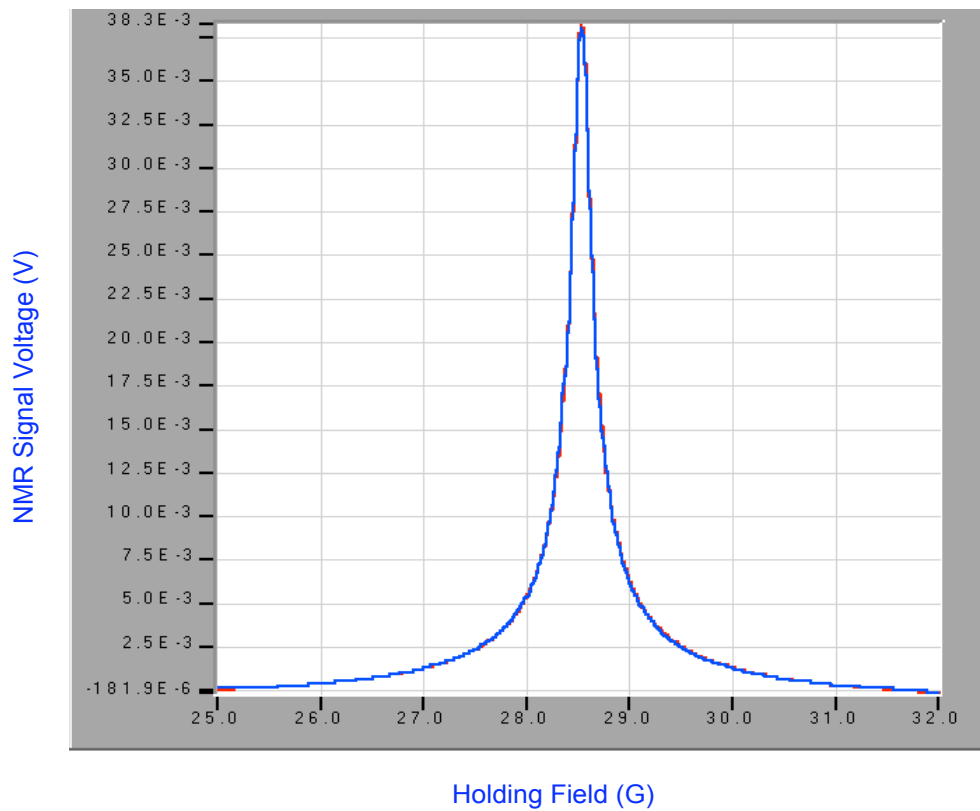


Figure 7: Up Sweep AFP Polarization Signal fit for Voltaire
Note: The data is marked in blue and the fit is marked in red.

Chapter 4

Water Calibration

4.1 Spin Relaxation

While the peak height of an NMR signal is a relative measure of polarization, it does not indicate the absolute value of the polarization. In order to calculate the absolute polarization the target system must be calibrated. Water serves as a good standard for calibrating the system because it has a known Boltzmann polarization.

In order to calibrate the system, a target cell is filled with de-ionized water and mounted between the pickup coils. The constant holding field and the oscillating RF field are applied and the system is swept at a rate of $1.2 \frac{G}{s}$. The holding field is ramping from 18 G to 25 G and is held at 25 G so that the spins relax. The water signal is swept from 18 G to 25 G rather than 25 G to 32 G because water and ^3He have different gyromagnetic ratios. The gyromagnetic ratio for the proton in water is $\gamma = 26752 \frac{\text{Hz}}{\text{G}}$, which means that in the presence of an RF field with a frequency of 91 kHz, the system passes through resonance around 21 G [14].

The spin relaxation rate of the proton is around 3 seconds and is on the order of the sweep rate [13]. Holding the magnetic field at 25 G allows the protons to depolarize back to their original spin state. When the field is ramped back down from 25 G to 18 G

the proton spins flip again. In short, the magnetizations flip, depolarize, and then flip again. The magnetic field is not held when a ^3He sample is tested because the depolarization time of ^3He is not on the order of the sweep rate; ^3He depolarizes much slower than water. Since the effects of spin relaxation are significant for the water sample they should be discussed. The magnetization in the \hat{z} direction relaxes in a manner described by

$$\frac{dM_z}{dt} = \frac{(M_z - M_0)}{T_1} \quad (4.1)$$

where M_z is the longitudinal component of the magnetization and M_0 represents the longitudinal component at thermal equilibrium. The magnetization in the \hat{x} direction and the \hat{y} direction relaxes as follows

$$\frac{dM_x}{dt} = -\frac{M_x}{T_2} \quad (4.2)$$

$$\frac{dM_y}{dt} = -\frac{M_y}{T_2} \quad (4.3)$$

Since the magnetization is proportional to the sum of the magnetic dipole moments, the precession of the effective magnetic field can be restated to include the relaxation effects [8, 12, 13].

$$\frac{\partial \vec{M}}{\partial t} = \vec{M} \times H_0 \hat{z} + H_1 \hat{x} \times \vec{M} - \frac{M_x}{T_2} \hat{x} - \frac{M_y}{T_2} \hat{y} - \frac{(M_z - M_0)}{T_1} \hat{z} \quad (4.4)$$

When equation (4.4) is written in terms of each coordinate. The resulting equations describe the magnetization of the water sample in the rotating frame and are called the Bloch equations

$$\frac{dM_x}{dt} = \gamma M_y H_0 \left[\frac{\gamma}{\omega} \right] \frac{M_x}{T_2} \quad (4.5)$$

$$\frac{dM_y}{dt} = \gamma M_z H_1 \left[\gamma M_x H_0 \right] \left[\frac{\gamma}{\omega} \right] \frac{M_y}{T_2} \quad (4.6)$$

$$\frac{dM_z}{dt} = \gamma M_y H_1 \left[\frac{(M_z - M_0)}{T_1} \right] \quad (4.7)$$

When the system is at resonance the proton spin flips in the water molecules. The maximum amplitude of the proton signal is [13]

$$S_w = \mu \gamma_w n_w P_w \left[\frac{geo}{w} \right] G_w \quad (4.8)$$

when γ_w is the magnetic moment of the proton, n_w is the density of the water sample, P_w is the polarization of water, $\left[\frac{geo}{w} \right]$ is the geometric flux factor that accounts for the cell geometry and cell placement between the pickup coils, G_w is the electronic gain in the system during the water measurement.

Since the same system is used for both the ^3He measurement and the water measurement the ratio of signals, $S_{^3\text{He}}$ to S_w can be made. This allows for the polarization of the ^3He sample to be calculated.

$$P_{^3\text{He}} = P_w \frac{\gamma_w}{\gamma_{^3\text{He}}} \frac{n_w}{n_{^3\text{He}}} \frac{G_w}{G_{^3\text{He}}} \left[\frac{geo}{w} \right] \frac{S_{^3\text{He}}}{S_w} \quad (4.9)$$

Every variable on the right side of equation (4.9) can be calculated or measured so that the polarization of ^3He can be determined.

4.2 Polarization of Water

The polarization of water can be calculated using a Boltzmann distribution function. The polarization is defined as

$$P = \frac{N_{\uparrow} - N_{\downarrow}}{N_{\uparrow} + N_{\downarrow}} \quad (4.10)$$

where N_{\uparrow} is the fraction of spins that are pointing parallel with the magnetic field, and N_{\downarrow} is the fraction of spins pointing anti-parallel to the magnetic field. The fraction of spins in any given state is [15]

$$N(i) = \frac{e^{-\frac{E_i}{kT}}}{Z} \quad (4.11)$$

where N is the fraction of spins pointing in a direction i , E_i is the energy, k is Boltzmann's constant ($k = 1.38 \times 10^{-23} \frac{J}{K}$) [16], T is the temperature in Kelvin, and Z is the partition function given by

$$Z(T) = \sum_i e^{-\frac{E_i}{kT}} \quad (4.12)$$

Combining equation (3.17) and equation (3.19) the energy is

$$E = \mp \frac{\hbar\omega}{2} \quad (4.13)$$

with $\omega = 2\pi \times 91$ kHz. The fraction of the spins that are parallel and anti-parallel with the magnetic field are then

$$N_{\uparrow} = \frac{e^{-\frac{\hbar\omega}{2kT}}}{e^{-\frac{\hbar\omega}{2kT}} + e^{\frac{\hbar\omega}{2kT}}} \quad (4.14)$$

$$N_{\uparrow} = \frac{e^{\frac{\hbar\omega}{2kT}}}{e^{\frac{\hbar\omega}{2kT}} + e^{-\frac{\hbar\omega}{2kT}}} \quad (4.15)$$

The polarization is then

$$P = \frac{e^{\frac{\hbar\omega}{2kT}} - e^{-\frac{\hbar\omega}{2kT}}}{e^{\frac{\hbar\omega}{2kT}} + e^{-\frac{\hbar\omega}{2kT}}} \quad (4.16)$$

$$P = \tanh\left(\frac{\hbar\omega}{2kT}\right) \quad (4.17)$$

Since $\hbar = 1.05 \times 10^{-34} \text{ J}\cdot\text{s}$ and $T = 295 \text{ K}$, the polarization of water is,

$$P_w \approx 7.3736 \times 10^{-9}.$$

4.3 Magnetic Moment and Electrical Gain

The magnetic moment of ^3He is $-2.1274 \mu_N$ [9] where

$\mu_N = 3.152454 \times 10^{-14} \frac{\text{MeV}}{T}$ [14]. The magnetic moment of protons in water is

$\mu_w = \mu_p = 2.79285 \mu_N$ [9]. The electronic gain refers to the gain on the preamplifier.

When performing NMR on a ^3He sample the gain is set at 10x. When performing NMR on a water sample the gain is set at 100x.

4.4 Flux Factor

4.4.1 Geometric Flux

In order to calibrate the NMR system an AFP polarization curve is generated for both a ^3He target cell and a water cell. Although every effort is made to make these two experiments identical, differences in cell geometry and cell placement between the pickup coils cannot be ignored. As the magnetization precesses at resonance its magnetic field, \vec{B} passes through the pickup coils. This field creates a flux [17].

$$\Phi = \oint \vec{B} \cdot d\vec{a} \quad (4.18)$$

However, as the magnetization precesses, the magnetic field changes with time, and as a result the flux varies with time. This change in flux induces an EMF in the pickup coils

$$EMF = - \frac{d}{dt} \oint \vec{B} \cdot d\vec{a} \quad (4.19)$$

The flux can also be written in terms of the magnetic vector potential, \vec{A} [17]

$$\oint \vec{B} \cdot d\vec{a} = \oint (\nabla \times \vec{A}) \cdot d\vec{a} = \oint \vec{A} \cdot d\vec{l} \quad (4.20)$$

In this form, rather than integrating over the area enclosed by the wire on the pickup coil, the magnetic vector potential is integrated around the path around the pickup coil.

Since each precessing ^3He nucleus is treated as a magnetic dipole with moment $\mu_{^3\text{He}}$, the vector potential from a certain point in the cell can be reduced to the dipole term of the multipole expansion [17]

$$\vec{A}_{dip}(\vec{r}) = \frac{\mu_0}{4\pi} \oint \frac{\mu \hat{r}}{r^2} d\Omega \quad (4.21)$$

where r is the distance from a specific magnetic dipole moment in the cell to a point on the path around the pickup coil. Combining equation (4.20) and equation (4.21) [18]

$$\Phi = \frac{\mu_0}{4\pi} \oint_C \int_V \frac{\vec{m} \cdot \vec{r}}{r^3} dV d\vec{l} \quad (4.22)$$

Since we calculate ratio of the ^3He signal to the water signal the factor $\frac{\mu_0}{4\pi}$ cancels out.

The magnetic moment is accounted for in equation (3.40) and equation (4.8) and as a result it can be pulled out of equation (4.22). Thus the geometric flux factor accounts for only geometric changes between the ^3He and the water signal.

$$\Phi^{geo} = \oint_C \int_V \frac{\vec{m} \cdot \vec{r}}{r^3} dV d\vec{l} \quad (4.23)$$

In order to calculate for the geometric flux, a C++ computer program was written that integrates the path around each coil. For points around the coil the magnetic vector potential due to points throughout the cell was calculated and summed together to calculate the total flux.

4.4.2 Coil Modeling

Researchers at the College of William and Mary work in close cooperation with researchers at the Thomas Jefferson National Accelerator Facility. Since input parameters for the flux code are used at both William and Mary and TJNAF it was necessary to model the pickup coils using a coordinate system that is consistent with the system used at TJNAF (*Figure 8*).

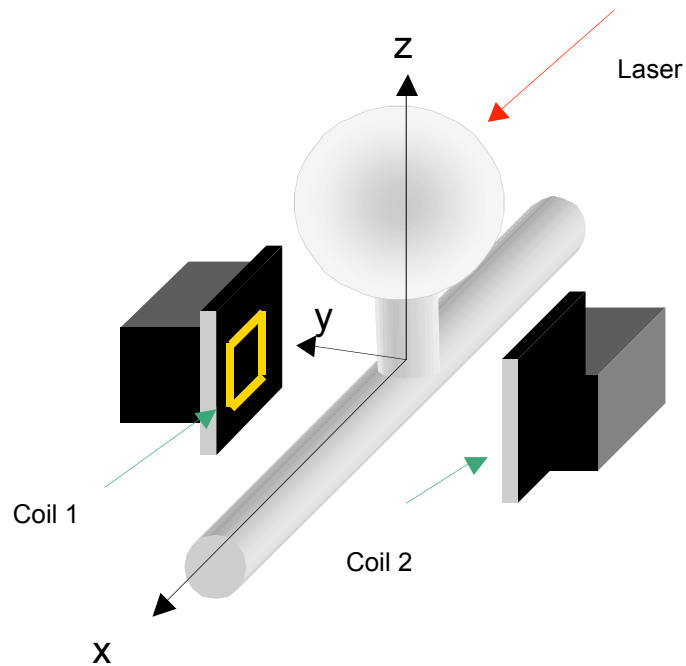


Figure 8: Coordinate System for Coil Modeling

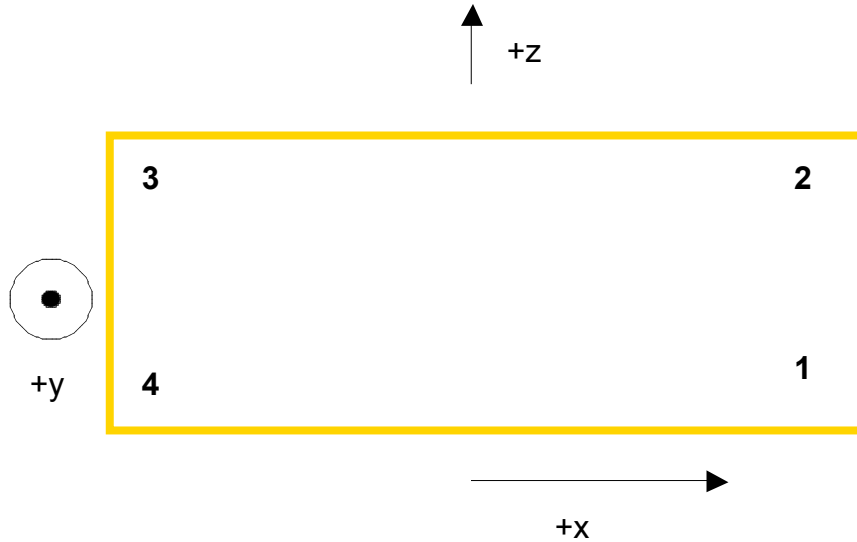


Figure 9: Coil Model

The dimensions of each of the four corners of the pickup coil are measured so that the distance between a volume element in the cell and a point on the coil can be measured.

In order to integrate around the coil, each coil was marked with four points, one at each corner. The corners were numbered as if one is looking from the +y direction at the cell (*Figure 9*).

The flux program begins by opening an input file specific to each cell. The input file contains all the necessary information regarding the cell dimensions, the pickup coil dimensions, and the location of the cell between the pickup coils. All coordinates are measured from the center of the target chamber of the cell. The top of the coil was divided up into 100 segments and the sides were divided up into 20 segments. The program first moved from point 3 to point 2 (the top of the coil) one segment at a time. The target chamber, transfer tube, and pumping chamber were divided up into 40 units in

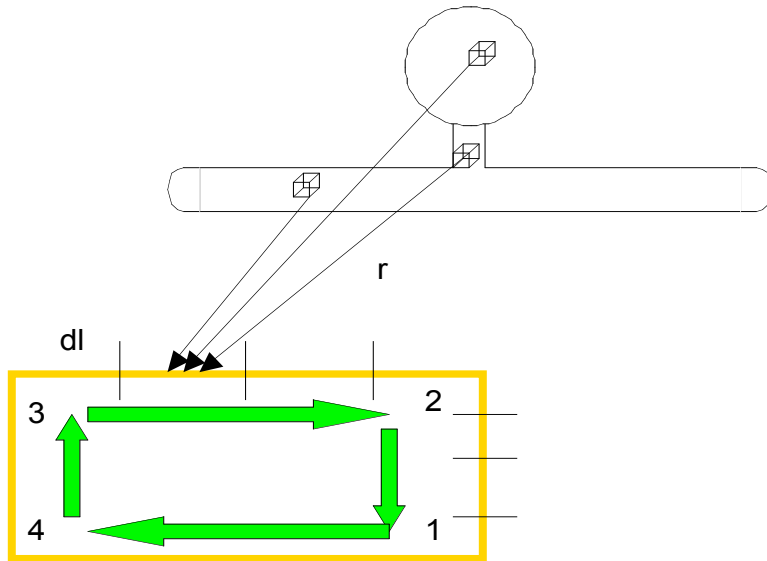


Figure 10: Calculating the geometric flux

In order to calculate the geometric flux the contribution from a number of volume elements in the target cell is summed for a number of points around the pickup coil. The summation loops around the pickup coils in the direction indicated by the green arrows above.

the x , y , and z directions. Each volume element was a box with dimensions determined by the size of the segments in each direction. The program calculated the magnetic vector potential from each volume element to the center of each segment on the coil. The total was stored in an array so that the effect on each point on the coil mesh could be analyzed. The process was repeated for all sides of coil 1 and coil 2 (*Figure 10*). Although every attempt was made to center the cell between the coils, there were slight misalignments. This was accounted for in the input file and during the integration.

	X	Y	Z
Coil	100		20
Target Chamber	40	40	40
Transfer Tube	40	40	40
Pumping Chamber	40	40	40

Table 1: Number of divisions in the target chamber, transfer tube, and pumping chamber

	Target Chamber Flux (cm²)	Transfer Tube Flux (cm²)	Pumping Chamber Flux (cm²)
Coil 1	20.8	0.4	-1.7
Coil 2	-23.7	-0.3	1.7
Total	44.5	0.7	-3.4

Total Flux: 41.8 cm²

Table 2: Voltaire Flux Results

Note: Since the coils face opposite directions the results from coil 1 are subtracted from the results of coil 2.

	Target Chamber Flux (cm²)	Transfer Tube Flux (cm²)	Pumping Chamber Flux (cm²)
Coil 1	24.3	0.5	-1.7
Coil 2	-24.7	-0.4	1.7
Total	49.1	0.9	-3.4

Total Flux: 46.1 cm²

Table 3: Water Cell Flux Results

Note: Since the coils face opposite directions the results from coil 1 are subtracted from the results of coil 2.

4.5 Measuring a Water Signal

A water signal was measured using the techniques of adiabatic fast passage. The density of the water in the cell was , $n_w = 2482 \text{ amg}$ [8]. The magnetic field was ramped from 18 G to 25 G and then back down again (*Figure 11*). Since water produces a weak signal, 400 sweeps were performed in an attempt to cancel out background noise. The signal was then fit by a computer program (*Figure 12*). The fit accounted for five parameters: signal height, holding field, resonance frequency, background slope, and background offset. From the fit it was determined that the signal height for the water sample was $(1.26 \pm 0.11) \times 10^{15} \text{ V}$.

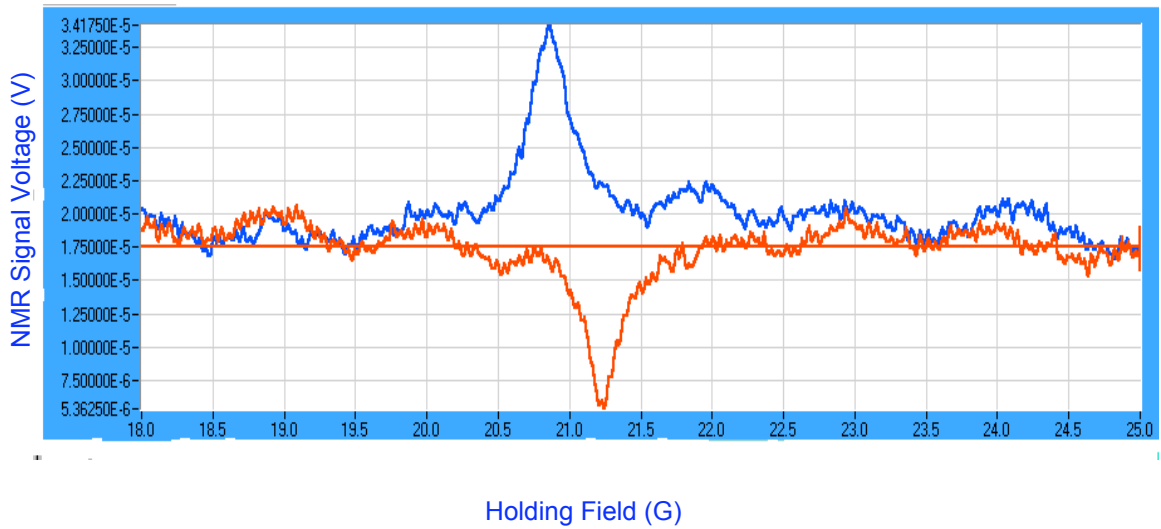


Figure 11: AFP Polarization Signal for Water Cell

Note: The up sweep is outlined in red and the down sweep is outlined in blue

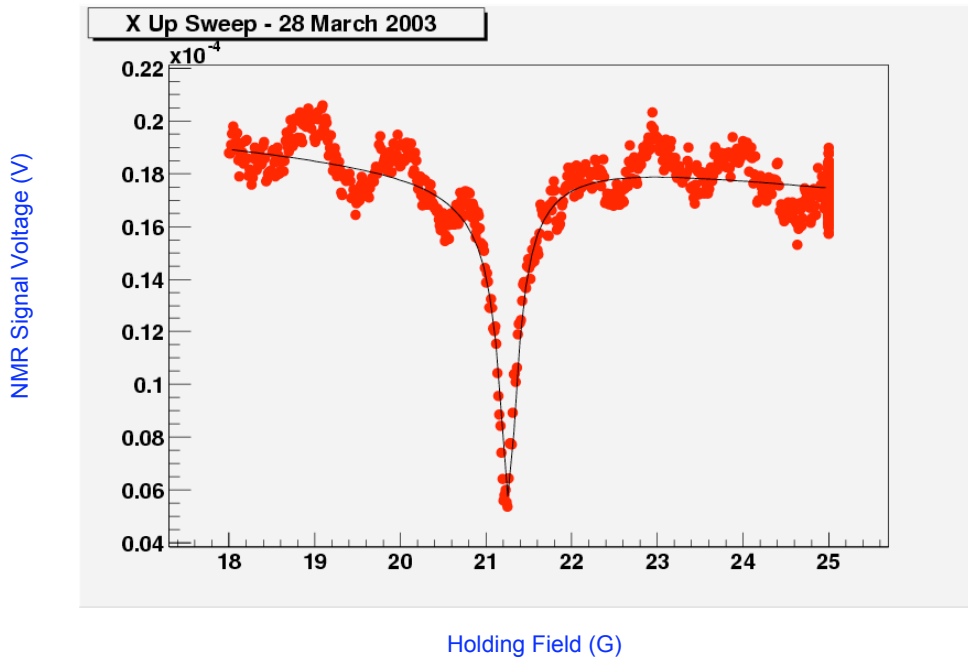


Figure 12: AFP Polarization Signal Fit for Water Sample

The side peaks are background noise.

4.6 Calibrating the System

Once the values on the right side of equation (4.9)

$$P_{^3\text{He}} = P_w \frac{\bar{\mu}_w}{\bar{\mu}_{^3\text{He}}} \frac{n_w}{n_{^3\text{He}}} \frac{G_w}{G_{^3\text{He}}} \frac{\bar{\mu}_w^{geo}}{\bar{\mu}_{^3\text{He}}^{geo}} \frac{S_{^3\text{He}}}{S_w} \quad (4.9)$$

are known, the polarization of a ^3He sample can be calculated. The values specific to the system at the College of William and Mary are summarized in *Table 4*.

Parameter	Value
P_w	7.37×10^{19}
$\bar{\mu}_w$	$2.79 \mu_N$
$\bar{\mu}_{^3\text{He}}$	$\approx 2.12 \mu_N$
n_w	2482 amg
$n_{^3\text{He}}$	10.2 amg
G_w	100
$G_{^3\text{He}}$	10
$\bar{\mu}_w^{geo}$	46.1 cm^2
$\bar{\mu}_{^3\text{He}}^{geo}$	41.8 cm^2
$S_{^3\text{He}}$	$39.5 \times 10^{13} \text{ V}$
S_w	$\approx 1.26 \times 10^{15} \text{ V}$

Table 4: Parameters used to calibrate an NMR system

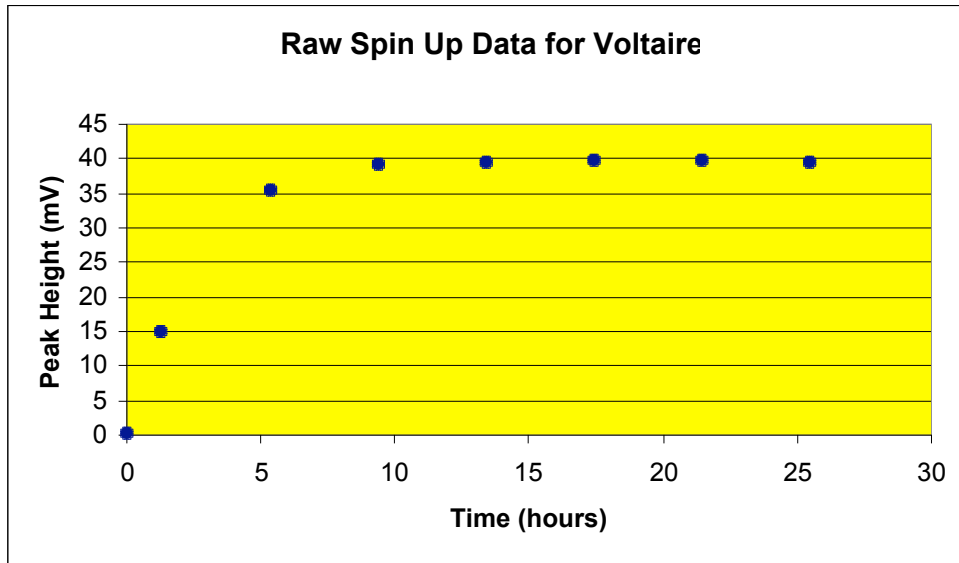


Figure 13: Spin up data for Voltaire.

The plot shows the peak height increasing over time for the AFP polarization signal measured for Voltaire. The plot includes data from when the sweep began until the peak height leveled off at its maximum value.

When the values in *Table 4* are inserted into equation (4.9) the maximum polarization of ^3He in Voltaire can be calculated, $P_{^3\text{He}} = 0.081 = 8.1\%$. The increase in the peak height and the increase in the polarization over time are shown in *Figure 13* and *Figure 14* respectively.

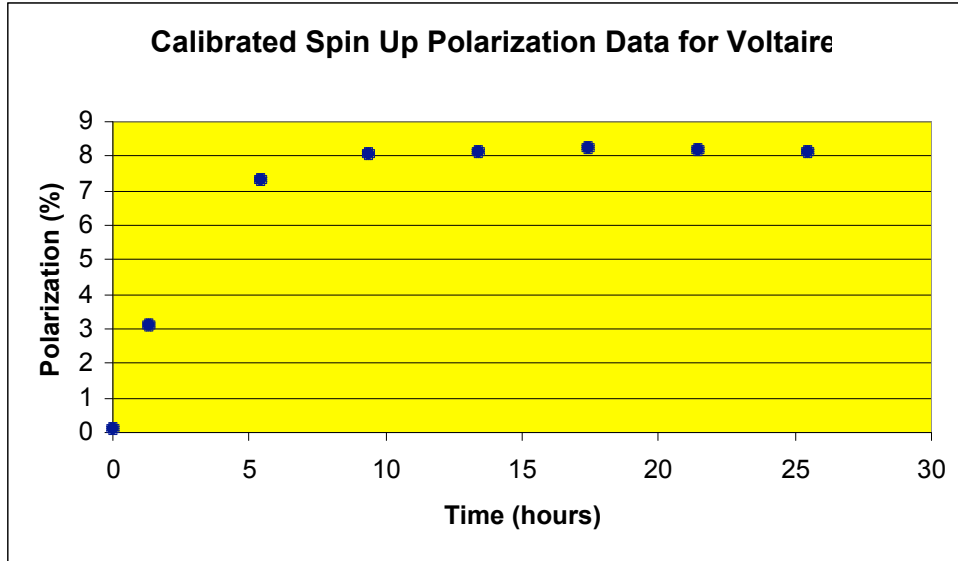


Figure 14: Spin up polarization data for Voltaire.

This plot shows the absolute polarization in percent vs. time for Voltaire. The plot includes data from when the sweep began until it leveled off at its maximum value.

4.7 Treatment of Errors

In this calibration there was error associated with measuring $n_{^3\text{He}}$, $S_{^3\text{He}}$, and S_w . In addition, error must be taken into account when calculating $\square_{^3\text{He}}^{geo}$ and \square_w^{geo} (Table 5). As discussed earlier, Voltaire was filled with 8.5 amg of ^3He . However, when the pumping chamber was heated during the optical pumping process the pressure in the target chamber changed to about 10.2 amg. When calculating this change in pressure, it was necessary to measure the interior volume of the cell. Due to some uncertainty in this volume measurement, $n_{^3\text{He}}$ has an error of about 5 %.

The signal height for Voltaire was fit using computer software. The error associated with this fit is approximately 1 %. The water signal is much weaker than the

^3He signal and as a result background noise made it difficult to fit. The water signal fit has an error of 9.0%.

Parameter	Error
$n_{^3\text{He}}$	5%
$S_{^3\text{He}}$	1%
S_w	9%
$\square_{^3\text{He}}^{geo}$	5%
\square_w^{geo}	5%
$P_{^3\text{He}}$	12.5%

Table 5: The errors in the water calibration of Voltaire

When calculating the flux (for both ^3He cells and water cells), inaccurate measurements in the input file are the largest source of error. The distance from the target cell to the pickup coils must be measured accurately because variations on the order of a millimeter can have a drastic effect on the total flux. Varying the number of divisions along the coil and in the cell has little impact on the flux (except when the number of divisions is set lower than 10). When the divisions along the coil were altered so that there were 50 divisions in the x direction and 10 in the z direction, and the size of the volume element in the cell remained unchanged, the total flux was 41.8 cm^2 , only a 0.001% change from the flux in *Table 2*. When the divisions along the coil were kept at

their original values (100 divisions in the x direction and 20 divisions in the z direction) and each chamber of the cell was divided up into 20 divisions rather than 40, the flux changed by only 1.8%. Due to measurement errors and the choice of segment size, it can be approximated that there is a 5% error associated with each calculation of the geometric flux. The total ^3He polarization error is approximately 12.5%.

Chapter 5

Conclusions

The goal of this Honors Project was to calibrate the NMR system at the College of William and Mary so that the absolute polarization of a ^3He sample could be measured. This goal was accomplished; the absolute polarization of the ^3He cell, Voltaire, was measured to be $(8.1 \pm 1.0)\%$. The research conducted in this project will help future researchers at the College of William and Mary measure the polarization of ^3He target cells.

The NMR research conducted this year at the College of William and Mary has focused on the pickup coils adjacent to the target chamber. Recently, however, upper coils were installed in the target system at William and Mary. These coils are circular and are adjacent to the pumping chamber of the cell. This year a flux code was also written for the upper coils, but this code has not yet been tested or debugged and more research is necessary before the measurements from these coils can be fully understood.

Appendix

The computer code used to calculate the geometric flux is on the pol3he computer in Small Hall in the directory named “marc” (~marc/flux.cc). The input file for Voltaire is located in ~marc/voltaire.dat, and the input data for the water cell is located in ~marc/watercell1.dat.

References

- [1] Tim Beardsley. Seeing the Breadth of Life. *Scientific American*. 1999.
- [2] B.G. Yerozolimsky, Nucl. Instr. and Meth. in Phys. Res. A **440**, 491 (2000).
- [3] I. Kominis, Measurement of the Neutron (^3He) Spin Structure at Low Q^2 and the Extended Gerasimov-Drell-Hearn Sum Rule, Princeton University, (2001).
- [4] T. Averett and W. Korsch, Thomas Jefferson National Accelerator Facility Proposal E97-103, <http://hallaweb.jlab.org/physics/experiments/he3/>
- [5] N. Liyanage, J.P. Chen, S. Choi, Thomas Jefferson National Accelerator Facility Proposal E01-012, <http://hallaweb.jlab.org/physics/experiments/he3/>
- [6] J.P. Chen, A. Deur, F. Garibaldi, Thomas Jefferson National Accelerator Facility Proposal E97-110, <http://hallaweb.jlab.org/physics/experiments/he3/>
- [7] D. Milkie, Polarization and Polarimetry of ^3He , College of William and Mary, (2002).
- [8] M.V. Romalis, Laser Polarized ^3He Target Used for a Precision Measurement of the Neutron Spin Structure, Princeton University, (1997).
- [9] T. Smith, A Precision Measurement of the Neutron Spin Structure Functions Using a Polarized ^3He Target, University of Michigan, (1998).
- [10] J.L. Knowles, Investigation of Techniques for Producing High Polarization ^3He Gas Targets, College of William and Mary, (1999).
- [11] D. Griffiths, Introduction to Quantum Mechanics, Prentice Hall, 1995.
- [12] A. Abragam, Principles of Nuclear Magnetism, Oxford University Press, 1999.
- [13] V.R. Pomeroy, Spin-Exchange Polarized ^3He Using Optically Pumped Alkali Atoms for Magnetic Resonance Imaging and Neutron Spin-Filters, University of New Hampshire, (1992).
- [14] X. Zheng, Precision Measurement of Neutron Spin Asymmetry A_1^n by large x_{Bj} Using CEBAF at 5.7 GeV, Massachusetts Institute of Technology, (2002).
- [15] C. Kittel, H. Kroemer, Thermal Physics, W.H. Freeman and Company, 1980.

- [16] P. Fishbane, S. Gasiorowicz, S. Thornton, Physics for Scientists and Engineers, Volume II, Prentice Hall, 1996.
- [17] D. Griffiths, Introduction to Electrodynamics, Prentice Hall, 1999.
- [18] S. Incerti, Calculation of the flux induced by a magnetized water cell, E94010 Technical Note 27, Jefferson Lab, (1999).